agriculture

MDPI

Article

Application of Exogenous 24-Epibrassinolide at the Silking Stage Alleviates the Effects of Post-Silking Heat Stress on Photosynthetic Performance of Waxy Maize

Jiawei Liu [1], Jing Li [1], Jian Guo [1], Huan Yang [1], Guanghao Li [1] and Dalei Lu [1,2,*]

[1] Jiangsu Key Laboratory of Crop Genetics and Physiology, Jiangsu Co-Innovation Center for Modern Production Technology of Grain Crops, Agricultural College of Yangzhou University, Yangzhou 225009, China; mx120230741@stu.yzu.edu.cn (J.L.); jli3260@sdau.edu.cn (J.L.); jianguo90@yzu.edu.cn (J.G.); huanyang@yzu.edu.cn (H.Y.); guanghaoli@yzu.edu.cn (G.L.)

[2] Joint International Research Laboratory of Agriculture and Agri-Product Safety, The Ministry of Education of China, Yangzhou 225009, China

* Correspondence: dllu@yzu.edu.cn

Abstract

Heat stress (HS) during the grain-filling stage severely limits yield in waxy maize by impairing leaf physiology and suppressing photosynthetic capacity. Although exogenous brassinosteroids are recognized for enhancing thermotolerance, their specific role in sustaining photosynthetic performance in waxy maize under HS has not been thoroughly investigated. This study investigated whether exogenous 24-epibrassinolide (BR) application could alleviate HS-induced damage in two waxy maize hybrids. Plants were exposed to HS with/without BR treatment over two growing seasons. Yield components, photosynthetic parameters, chloroplast ultrastructure, antioxidant enzyme activities, and physiological traits were analyzed. HS during the grain-filling stage significantly reduced maturity yields (SYN5: −42.8%; YN7: −39.0%) by impairing photosynthetic efficiency, chloroplast integrity, antioxidant capacity, and the translocation amount and rate of vegetative organs photosynthate after pollination. Chloroplasts exhibited structural disorganization and pronounced swelling. Photosynthetic pigment content and enzyme activities (ribulose-1,5-bisphosphate carboxylase/oxygenase, phosphoenolpyruvate carboxylase) declined, while reactive oxygen species accumulation increased. Exogenous BR substantially restored yields by preserving the chloroplast ultrastructure, enhancing photosynthetic function, reactivating antioxidant enzymes (ascorbate, catalase, superoxide dismutase), and reducing oxidative damage. BR also optimized hormone balance (reduced abscisic acid, increased indole-3-acetic acid) and elevated soluble protein/sugar contents. Meanwhile, BR reversed the negative effects of HS on dry matter accumulation and translocation. SYN5 suffered greater HS damage but exhibited stronger BR-mediated recovery than YN7. In conclusion, BR application mitigates HS by protecting the chloroplast structure, boosting photosynthetic resilience, and activating antioxidant defenses, offering a strategy to safeguard waxy maize productivity under HS.

Keywords: brassinosteroids; heat stress; photosynthetic performance; waxy maize

check for updates

Academic Editor: Anshu Rastogi

Received: 28 October 2025
Revised: 19 November 2025
Accepted: 23 November 2025
Published: 26 November 2025

Citation: Liu, J.; Li, J.; Guo, J.; Yang, H.; Li, G.; Lu, D. Application of Exogenous 24-Epibrassinolide at the Silking Stage Alleviates the Effects of Post-Silking Heat Stress on Photosynthetic Performance of Waxy Maize. *Agriculture* **2025**, *15*, 2445. https://doi.org/10.3390/agriculture15232445

Copyright: © 2025 by the authors. Licensee MDPI, Basel, Switzerland. This article is an open access article distributed under the terms and conditions of the Creative Commons Attribution (CC BY) license (https://creativecommons.org/licenses/by/4.0/).

1. Introduction

The global mean temperature has risen by 1.2 °C over the past decade with projections indicating it will exceed 1.5 °C by 2040 [1]. Such warming triggers cascading environmental

disruptions that severely compromise crop phenology and geographic distribution [2,3]. Under future climate scenarios, heatwaves are predicted to intensify in both frequency and severity [4]. Extensive evidence confirms that cereal crops, particularly maize (*Zea mays* L.), suffer profound yield penalties under heat stress (HS) [5,6]. Critically, each 1 °C rise in global temperature reduces maize yields by 7.4% [7,8], threatening global food security. Furthermore, sustained temperatures above the 35 °C threshold can cause irreversible damage to maize [9].

Waxy maize (*Zea mays* L. var. *ceratina* Kulesh), a key specialty crop, carries a recessive mutation in the *waxy* gene, resulting in endosperm starch composed predominantly of amylopectin [10]. Its distinctive gelatinization and digestibility properties have established broad industrial utility across food processing, chemical manufacturing, and biomedical sectors [11,12]. However, the production stability of this vital crop is increasingly threatened by intensifying HS, which is a major challenge under escalating global temperatures [13].

As the primary organ of photosynthesis, leaves are fundamental to yield formation and stress responses [14,15]. HS severely constrains crop productivity by disrupting leaf physiological functions, particularly photosynthesis [16]. It directly damages photosystem II (PSII), impairing its structural integrity and reducing photosynthetic efficiency [17,18]. Concurrently, the HS-triggered suppression of antioxidant defenses leads to ROS accumulation [19,20], which induces oxidative damage to membranes and DNA, promoting cell death [21]. HS also disrupts osmotic balance, depleting key osmolytes [22,23]. Consequently, these perturbations upregulate senescence-associated genes [24], thereby accelerating leaf senescence and imposing significant yield losses [25]. Identifying interventions to delay this HS-driven senescence is thus essential for protecting waxy maize yield.

Brassinosteroids (BRs), a class of multifunctional phytohormones [26], enhance crop tolerance by modulating the antioxidant system, stabilizing the photosynthetic apparatus, and balancing endogenous hormone levels [27,28]. BRs do not function in isolation but engage in complex crosstalk with other hormonal pathways to orchestrate stress adaptation. In cereal crops, BRs and abscisic acid (ABA) collaborate to regulate carbohydrate metabolism and membrane stabilization under low-temperature stress [29]. BR signaling also correlates positively with auxin levels, as shown in tobacco, where BR-induced leaf growth coincides with elevated indole-3-acetic acid (IAA) and the synergistic upregulation of biosynthetic and signaling components [30]. Extensive studies confirm that BRs improve crop abiotic stress resistance through multiple mechanisms, including the BZR1-ROS signaling pathway in development and the expression of heat shock proteins under HS [31–34]. Studies document that BR mitigates HS-induced declines in photosynthetic efficiency through several mechanisms, including the following: augmenting leaf photosynthetic pigment content; stimulating initial ribulose-1,5-bisphosphate carboxylase/oxygenase (Rubisco) activity to enhance carboxylation; increasing PSI photochemical activity and energy charge; and enhancing PSII quantum efficiency [35–37]. However, the physiological mechanisms by which exogenous BR alleviates HS responses specifically in waxy maize leaves remain unclear.

Therefore, this study aimed to (1) elucidate the effects of exogenous BR on photosynthetic properties, antioxidant systems, endogenous hormone and osmoregulatory substance content, substance accumulation/translocation, and the yield of waxy maize leaves under HS during the grain-filling stage; and (2) investigate the physiological mechanisms by which exogenous BR maintains leaf photosynthetic performance under HS. These findings are expected to provide a theoretical foundation for applying exogenous BR to enhance HS tolerance and stabilize yield in waxy maize production.

2. Materials and Methods

2.1. Experiment Sites and Materials

The experiment was conducted during the periods of March to July in both 2023 and 2024 at the experimental field of Yangzhou University (Yangzhou, China, 32°39′42″ N, 119°41′29″ E). Two waxy maize hybrids, Suyunuo5 (SYN5, provided by the Jiangsu Yanjiang Institute of Agricultural Sciences, Nantong, China) and Yunuo7 (YN7, provided by the Chongqing Academy of Agricultural Sciences, Chongqing, China) were used in this study. The seeds were initially placed in seedling trays within the greenhouse, where they underwent the germination process. Subsequent to the completion of the first leaf development, the seedlings were transplanted into pots (height = 38 cm, diameter = 43 cm). The pots contained sieved loam soil with a weight of 39 kg. Additionally, 10 g of compound fertilizer ($N/P_2O_5/K_2O$ = 27%/9%/9%) was applied to each pot as basal fertilizer. At the jointing stage (6-leaf stage), the strongest seedling in each pot was retained, and 6.6 g of urea (N = 46%) was applied. Ambient temperature and precipitation data recorded before treatments in both years are presented in Figure S1.

Plants were field-grown until silking and artificially pollinated. They were then divided into two groups for foliar application: one was sprayed with a solution of 0.25 mg/L 24-epibrassinolide (BR, Yinzhihai Chemical Products Co., Ltd., Zhengzhou, China) containing 0.05% Tween-20 (Polyoxyethylene (20) sorbitan monolaurate, Sinopharm Chemical Reagent Co., Ltd., Beijing, China), and the other (control) received an equal volume of water. The BR concentration was based on a previous study by Gao et al. [38]. Following a 12-hour period of rest, the two groups of plants were transferred to an intelligent temperature-controlled glasshouse for a 15-day temperature treatment, including heat stress treatment (HS, day/night = 35 °C/28 °C) and control treatment (CK, day/night = 28 °C/20 °C). Therefore, this experiment contained four treatments: CK, HS, CKBR (CK together with BR), and HSBR (HS together with BR). The soil relative water content was maintained at approximately 75% by daily measuring pot weight loss and replenishing the evapotranspirative water loss accordingly. The temperature was restored to control levels post-treatment until physiological maturity.

2.2. Sampling, Measurement and Analysis

2.2.1. Yield Determination and Dry Matter Accumulation/Translocation

Three ears per treatment were sampled at maturity in both 2023 and 2024. Kernels were removed from the ears and dried to constant weight at 80 °C. The grain yield of per plant was calculated at a standardized moisture content of 14%.

For dry matter (DM) analysis, three plants per treatment were destructively sampled at both silking and maturity stages in 2023 and 2024. The plants were then divided at the silking stage into stem, leaf, sheath, and tassel, and then at the maturity stage they were divided into stem, leaf, sheath, tassel, cob, and grain. All samples were dried in a heating chamber at 80 °C until constant weight.

The parameters of dry matter accumulation and translocation were calculated by Wang et al. (2012) [39]:

$$\text{TAP} = \text{DM of vegetative organs at flowering stage} - \text{DM of vegetative organs at maturity} \quad (1)$$

$$\text{TRP (\%)} = 100 \times \text{TAP}/\text{DMF} \quad (2)$$

$$\text{CRP (\%)} = 100 \times \text{TAP}/\text{Grain dry weight at maturity} \quad (3)$$

$$\text{TAA (g/plant)} = \text{Grain dry weight at maturity} - \text{TAP} \quad (4)$$

$$\text{CRA (\%)} = 100 \times \text{TAA/Grain dry weight at maturity} \quad (5)$$

$$\text{DMA (g/plant)} = \text{DM of whole plant at maturity} - \text{DMF} \quad (6)$$

where TAP (g/plant): translocation amount of vegetative organ photosynthate before flowering, TRP (%): translocation rate of vegetative organ photosynthate before flowering, CRP (%): contribution rate of vegetative organ photosynthate before flowering to grain, TRP (%): translocation rate of vegetative organ photosynthate before flowering, TAA (g/plant): translocation amount of vegetative organ photosynthate after pollination, CRA (%): contribution rate of vegetative organ photosynthate after pollination to grain, DMA (g/plant): dry matter accumulation after flowering stage.

2.2.2. Photosynthetic Parameter Measurement

In 2024, photosynthetic gas exchange parameters of the ear leaf (the leaf subtending the primary ear) were measured using an LI-6400 portable photosynthesis system (LI-COR Biosciences, Lincoln, NE, USA). Measurements were taken between 09:00 and 11:00 AM at 5 and 15 days after pollination (DAP). Three plants per treatment were randomly selected for measurement on each date. The net photosynthetic rate (Pn), stomatal conductance (Gs), intercellular CO_2 concentration (Ci), and transpiration rate (Tr) of the middle section of the ear-leaf were measured.

2.2.3. Leaf Anatomical Microstructure Observation

Ear leaf segments (0.5 cm × 0.5 cm) from mid-lamina regions (veins excluded) were harvested at 15 DAP in 2024 and fixed in FAA (50% ethanol: 37–40% formaldehyde: glacial acetic acid = 90:5:5, *v*/*v*) overnight. Samples underwent ethanol dehydration (75%, 4 h; 85%, 2 h; 90%, 2 h; 95%, 1 h; 100%, 30 min × 2) and then wax infiltration via ethanol–benzene (5–10 min), xylene I/II (5–10 min each), and molten paraffin (65 °C, 1 h × 3). Tissues were embedded (JB-P5 station), solidified (−20 °C), and sectioned at 2–4 μm (Leica RM2016, Wetzlar, Germany). Sections were expanded (40 °C water bath), slide-mounted, baked (60 °C), dewaxed via xylene I/II (20 min each), ethanol series (absolute I/II: 5 min; 75%: 5 min), and rinsed (slow-running tap water, 5 min). After toluidine blue O staining (2–5 min) and deionized water rinse, intensity was assessed (Nikon Eclipse E100, Tokyo, Japan; destained in 70% ethanol if required). Finally, sections were oven-dried, cleared (fresh xylene, 5 min), resin-mounted, and examined (Leica DM1000, Wetzlar, Germany).

2.2.4. Mesophyll Cell Ultrastructure Observation

Samples matching 2.2.3 specifications underwent primary fixation in 2.5% glutaraldehyde/0.1 M PBS (pH 7.4, 4 °C, 12 h), after which they were rinsed in chilled PBS (15 min × 3) and then secondary fixed in 1% osmium tetroxide/PBS (pH 7.4, 20 °C dark, 2 h). After PBS rinses (15 min × 3), dehydration proceeded through graded ethanol (50%, 70%, 80%, 90%, 95%, 100% × 2; 15 min/step). Infiltration used 1:1 acetone: Spurr's resin (812 formulation, 12 h) then pure resin (12 h). Polymerization (60 °C, 48 h) preceded ultrathin sectioning (60–80 nm; Leica UC7, Wetzlar, Germany, Diatome Ultra 45° knife). Sections were double-stained with uranyl acetate (2%, 15 min) and Reynolds' lead citrate (15 min), air-dried, and imaged (FEI Tecnai G2 20 TWIN TEM, Hillsboro, OR, USA).

2.2.5. Photosynthetic Pigment, Osmotic Adjustment Substances Quantification

Ear leaf mid-sections were sampled at 5 and 15 DAP during both 2023 and 2024 with three replicates per treatment. The surface moisture was gently blotted. Photosynthetic pigments (chlorophyll a, b, carotenoids) were extracted and quantified spectrophotometrically following Arnon (1949) [40]. The contents of soluble protein and soluble sugar were quanti-

fied using commercial assay kits (YJ910347 for protein, ml076788 for sugar) from Shanghai Enzyme Link Biotechnology Co., Ltd. (Shanghai, China). The soluble protein content was determined based on the Coomassie Brilliant Blue G-250 binding method, while the soluble sugar content was assessed employing the anthrone–sulfuric acid colorimetric method.

2.2.6. Enzyme Activities, Peroxides, and Endogenous Hormones

Ear leaf mid-sections were sampled at 5 and 15 DAP during both 2023 and 2024 (n = 3 per treatment), immediately frozen in liquid nitrogen and stored at −80 °C until analysis. Activities of phosphoenolpyruvate carboxylase (PEPCase), ribulose-1,5-bisphosphate carboxylase/oxygenase (Rubisco), superoxide dismutase (SOD), peroxidase (POD), activities of catalase (CAT) and ascorbate (APX) were determined using commercial kits (YJ403921, YJ410725, YJ495037, YJ495039, YJ495038, YJ490381). Contents of reactive oxygen species (ROS), hydrogen peroxide (H_2O_2), abscisic acid (ABA), and indole-3-acetic acid (IAA) were quantified with kits YJ904081, ml076343, YJ077235, and YJ077231, respectively. All enzymatic activities (Rubisco, PEPCase, SOD, CAT, POD) and substance concentrations (H_2O_2, ROS, IAA, ABA) were determined using commercial kits based on the enzyme-linked immunosorbent assay (ELISA) principle. With the exception of APX, which was measured at 290 nm, the optical density (OD) for all other assays was read at 450 nm on an INFRNITE M Nano microplate reader (Switzerland). Quantification was achieved by interpolation from standard curves specific to each analyte, and all measurements were conducted with three replicates. All the kits were sourced from Shanghai Enzyme Link Biotechnology Co., Ltd. (Shanghai, China).

2.3. Statistical Analyses

Data organization used WPS Office (v12.1; Kingsoft Corp., Beijing, China). Significant differences among treatments ($p < 0.05$) were determined by one-way analysis of variance (ANOVA) followed by Tukey's HSD test in Data Processing System software (v7.05; Hangzhou Rui Feng Tech., Hangzhou, China). Figures were prepared using SigmaPlot (v14.0; Systat Software Inc., San Jose, CA, USA) and Adobe Illustrator CC2024 (v28.0; Adobe Inc., San Jose, CA, USA). Chloroplast structural data were analyzed using ImageJ (v1.52a; NIH., Bethesda, MD, USA).

3. Results

3.1. Maturity Yield

HS significantly reduced the maturity yield of both waxy maize hybrids. Exogenous BR application substantially mitigated this yield loss (Figure 1, Table S1). Compared to CK, the two-year average yields of SYN5 and YN7 decreased by 42.8% and 39.0%, respectively, under HS. Under HSBR treatment, yields increased by 35.3% (SYN5) and 20.4% (YN7) relative to HS. Notably, exogenous BR significantly increased SYN5 maturity yield under CK conditions in 2024 (Figure 1). YN7 consistently exhibited higher yields than SYN5 (Table S1). SYN5 suffered a greater yield reduction from HS but also achieved a stronger recovery with BR than YN7.

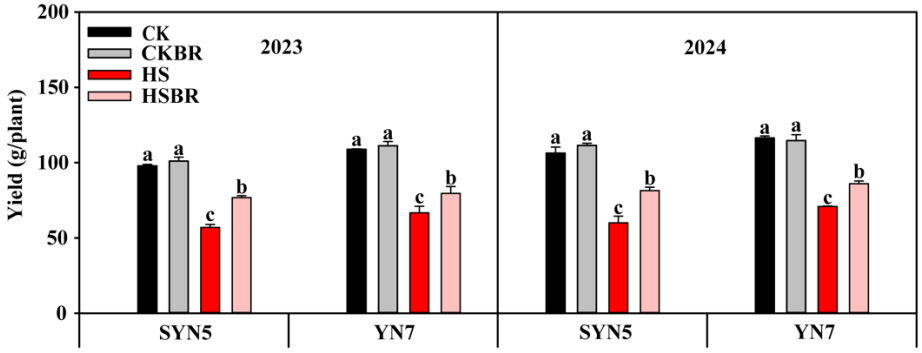

Figure 1. Effects of HS and BR on the yield of waxy maize. CK: control, HS: heat stress, BR: 24-epibrassinolide. Error line represents the standard deviation of the mean (n = 3). Different letters indicate significant differences ($p < 0.05$).

3.2. Dry Matter Accumulation and Translocation

In both years, HS significantly increased TAP, TRP, and CRP while significantly decreasing in TAA, CRA, and DMA in both waxy maize hybrids. Compared to CK, HS increased TAP, TRP, and CRP by 224.6%, 12.5%, and 45.5% in SYN5 and by 179.5%, 11.0%, and 38.4% in YN7. Conversely, HS decreased TAA, CRA, and DMA by 73.0%, 45.5%, and 63.8% in SYN5, and by 65.0%, 38.4%, and 57.5% in YN7. Dry matter accumulation and translocation were more affected in SYN5 under HS compared with YN7.

Exogenous BR application significantly mitigated these effects (Table 1 and Table S1). Relative to HS without BR, BR reduced TAP, TRP, and CRP by 15.9%, 4.7%, and 21.6% in SYN5 and by 26.2%, 5.0%, and 19.5% in YN7. BR increased TAA, CRA, and DMA by 103%, 21.6%, and 68.5% in SYN5 and by 70%, 19.5%, and 38.4% in YN7. Under CKBR in 2024, TAP and TRP significantly decreased while TAA increased in SYN5 compared to CK. Interannual comparisons revealed greater HS severity and BR effectiveness in 2023 compared to 2024 for both hybrids (Table S1).

Table 1. The impact of HS and BR on dry matter accumulation and translocation.

Year	Hybrid	Treatment	TAP (g/Plant)	TRP (%)	CRP (%)	TAA (g/Plant)	CRA (%)	DMA (g/Plant)
2023	SYN5	CK	8.5c	3.6c	10.3d	74.3b	89.7a	112.9b
		CKBR	9.0c	3.9c	10.5d	76.5b	89.5a	112.2b
		HS	26.9a	16.3a	56.1a	21.1e	43.9d	44.5d
		HSBR	20.8b	10.9b	32.1c	44.0c	67.9b	70.3c
	YN7	CK	9.0c	3.5c	9.7d	83.1a	90.3a	118.9ab
		CKBR	8.9c	3.5c	9.5d	85.3a	90.5a	121.2a
		HS	28.6a	15.1a	50.7b	27.7d	49.3c	52.1d
		HSBR	22.0b	10.5b	31.8c	47.7c	68.2b	72.9c
2024	SYN5	CK	11.8d	4.5e	13.1e	78.6b	86.9a	127.8b
		CKBR	8.9e	3.3f	9.4e	85.9a	90.6a	131.7b
		HS	29.6a	16.7a	58.2a	21.4f	41.8e	43.4e
		HSBR	27.0b	12.8c	39.0c	42.3d	61.0c	77.7c
	YN7	CK	12.0d	4.3ef	12.1e	87.0a	87.9a	138.3ab
		CKBR	10.6de	3.7ef	10.9e	86.9a	89.1a	143.6a
		HS	28.8ab	14.6b	47.9b	31.4e	52.1d	56.8d
		HSBR	20.3c	9.3d	27.8d	52.8c	72.2b	77.8c

TAP: translocation amount of vegetative organ photosynthate before pollination (g/plant), TRP: translocation rate of vegetative organs photosynthate before pollination (%), CRP: contribution rate of vegetative organs photosynthate before pollination to grain weight (%), TAA: translocation amount of vegetative organs photosynthate after pollination (g/plant), CRA: contribution rate of vegetative organs photosynthate after pollination to grain weight (%), DMA: dry matter accumulation after pollination (g/plant), CK: control, HS: heat stress, BR: 24-epibrassinolide. Means in the same column of a single variety followed by different letters are significantly different ($p < 0.05$).

3.3. Photosynthetic Parameters

HS substantially decreased Pn and Gs while notably increasing Ci and Tr at both 5 DAP and 15 DAP in both hybrids. Exogenous BR mitigated these effects (Figure 2). HS reduced Pn relative to CK to a greater extent in SYN5 (19.2% at 5 DAP; 22.0% at 15 DAP) than in YN7 (6.8% at 5 DAP; 9.8% at 15 DAP). Exogenous BR significantly enhanced Pn in SYN5 at 5 DAP under CK and at 15 DAP under HS. The alterations in Gs under HS and BR treatments followed a pattern analogous to that of Pn (Figure 2B). HS elevated Ci in SYN5 by 31.1% (5 DAP) and 37.6% (15 DAP), while increases for YN7 were 12.5% (5 DAP) and 55.1% (15 DAP) (Figure 2C). Exogenous BR significantly reduced Ci in both hybrids under HS except for YN7 at 5 DAP. Tr in both hybrids showed a trend similar to Ci under HS (Figure 2D). Exogenous BR significantly reduced Tr in SYN5 at 5 DAP under CK, and it substantially decreased Tr in both hybrids at 15 DAP.

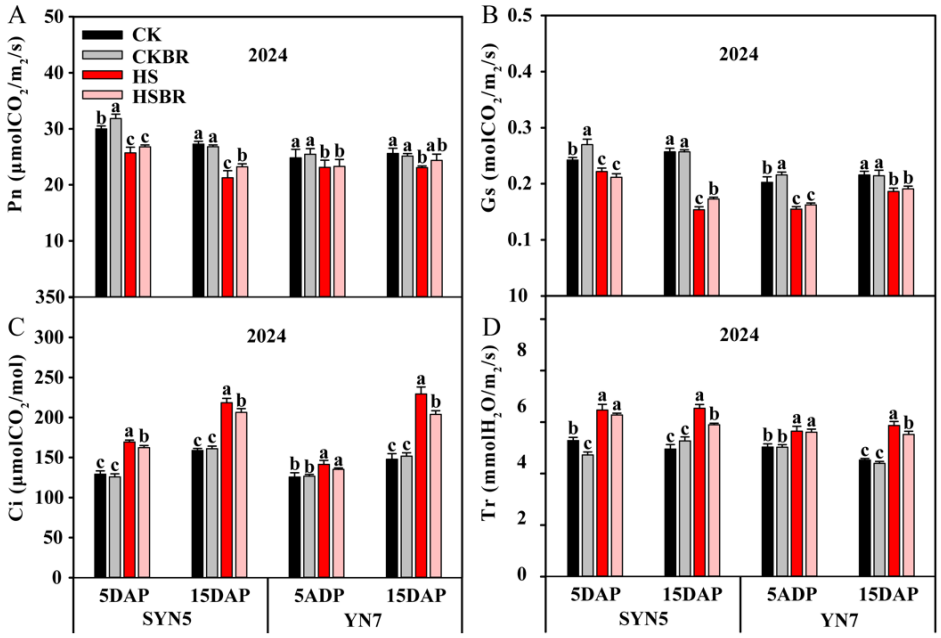

Figure 2. Effects of HS and BR on photosynthetic parameters of waxy maize. (**A**) Net photosynthetic rate (Pn), (**B**) stomatal conductance (Gs), (**C**) intercellular CO_2 concentration (Ci), (**D**) transpiration rate (Tr). DAP: days after pollination, CK: control, HS: heat stress, BR: 24-epibrassinolide. Different letters indicate significant differences ($p < 0.05$). Error line represents the standard deviation of the mean (n = 3).

3.4. Leaf Anatomical Microstructure

HS reduced both the number of mesophyll cells and the volume of wreath-like structures without a corresponding change in mesophyll cell size. (Figure S2). Furthermore, HS substantially decreased the leaf thickness, mesophyll thickness, vascular bundle tissue area, and bundle sheath tissue area. These detrimental effects were mitigated by exogenous BR application (Table 2, Figure S2). Compared to CK, HS induced significant reductions in various parameters of leaf thickness (35.1%), upper epidermis thickness (14.1%), lower epidermis thickness (20.2%), vascular bundle tissue area (64.4%), and vascular bundle sheath tissue area (44.4%) in SYN5. In contrast, YN7 exhibited lesser reductions under HS in leaf thickness (4.1%), mesophyll thickness (7.8%), vascular bundle area (77%), and bundle sheath area (13.7%), along with a 17.6% increase in upper epidermis thickness. Exogenous BR significantly increased the vascular bundle sheath tissue area in both hybrids. The HSBR treatment elevated the vascular bundle tissue area and bundle sheath tissue area by 39.2% and 13.2% in SYN5 and by 117.3% and 45.2% in YN7 relative to HS alone. Collectively, the

ear leaf anatomy of SYN5 was more severely impacted by HS but also exhibited a stronger restorative response to exogenous BR compared to YN7.

Table 2. Effects of HS and BR on the anatomical structure of waxy maize ear leaves.

Hybrid	Treatment	Leaf Thickness (μm)	Upper Epidermis Thickness (μm)	Under Epidermis Thickness (μm)	Mesophyll Thickness (μm)	Vascular Bundle Tissue Area ($μm^2$)	Bundle Sheath Tissue Area ($μm^2$)
SYN5	CK	239.0a	29.0a	25.7a	184.2a	2545.7a	7650.4b
	CKBR	235.9a	28.7a	27.8a	179.4a	2810.0a	9192.2a
	HS	155.2c	24.9b	20.5b	109.8b	906.8c	4250.8d
	HSBR	164.7b	26.6a	21.4b	115.0b	1262.0b	4810.2c
YN7	CK	212.9a	30.7b	23.2a	159.1ab	3233.2a	7876.3b
	CKBR	215.0a	27.5b	23.3a	164.3a	3265.6a	9251.9a
	HS	204.1b	36.1a	25.0a	143.0c	746.0c	6797.2c
	HSBR	205.4b	26.7b	25.8a	152.9b	2218.2b	9870.1a

CK: control, HS: heat stress, BR: 24-epibrassinolide. Means in the same column of a single variety followed by different letters are significantly different ($p < 0.05$).

3.5. Mesophyll Cell Ultrastructure

HS significantly altered the morphology and structure of chloroplasts in the mesophyll cells of both waxy maize hybrids (Figure 3), reducing the number of chloroplasts per mesophyll cell and the number of lamellae per grana (Table 3). Following HS treatment, chloroplasts per mesophyll cell and lamellae per grana decreased by 36% and 20%, 26.6% and 17.5% in SYN5 and YN7 compared to CK, respectively. Furthermore, the number of grana per unit area of chloroplast decreased by 54.5% in SYN5, while it increased by 11.7% in YN7. Chloroplasts in the mesophyll cells of both hybrids under CK exhibited normal morphology and adequate internal structure, manifesting as pike or ellipsoid shapes with intact outer envelopes and distinct boundaries. Basal lamellae were orderly stacked and lamellae tightly and clearly arranged. Under HS, the chloroplast membranes of SYN5 underwent evident solubilization, resulting in structural disintegration, loosening of the basal lamellae, solubilization of the grana lamellae, and obscured lamellae boundaries. In YN7, the outer membranes underwent partial solubilization, basal lamellae remained orderly arranged but with increased gaps, and lamellae boundaries became less distinct. Furthermore, chloroplast width and area increased significantly in both hybrids after HS treatment (Table 3). Chloroplasts appeared "edematous" and became ellipsoid or nearly round. These morphological changes were more pronounced in SYN5 than in YN7 (Figure 3).

Table 3. Effects of HS and BR on the ultrastructure of mesophyll cells of waxy maize ear leaves.

Variety	Treatment	Chloroplast per Mesophyll Cell	Chloroplast Size			Grana per Unit Area of Chloroplast ($μm^{-2}$)	Lamellae per Grana
			Length (μm)	Width (μm)	Area ($μm^2$)		
SYN5	CK	8.3ab	5.5a	4.4b	25.3c	1.2a	20.4bc
	CKBR	9.0a	5.2a	3.2c	22.9c	1.1a	28.5a
	HS	5.3b	5.6a	5.1a	34a	0.5b	15.0c
	HSBR	6.0b	5.5a	4.8a	29.8b	1.0a	26.0ab
YN7	CK	6.7a	5.3ab	4.5bc	24.7b	1.0a	22.9a
	CKBR	7.0a	5.5a	4.1c	24.9b	1.0a	25.0a
	HS	5.3b	5.4ab	5.2a	31.5a	0.7b	18.9b
	HSBR	5.7b	5.3b	4.7b	26.3b	0.9ab	22.1a

CK: control, HS: heat stress, BR: 24-epibrassinolide. Means in the same column of a single variety followed by different letters are significantly different ($p < 0.05$).

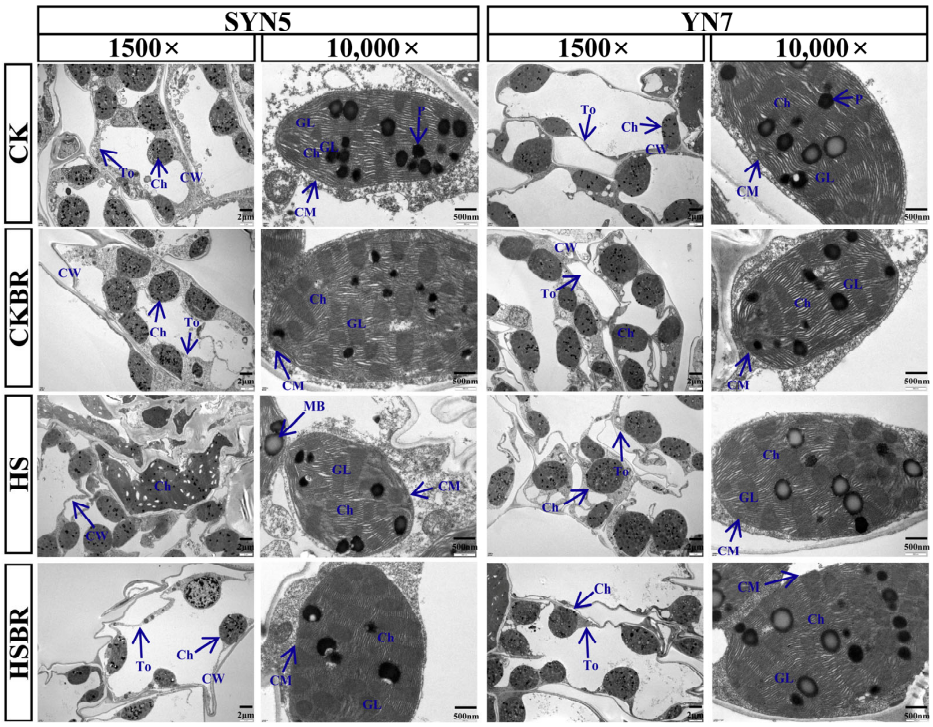

Figure 3. Transmission electron micrographs of mesophyll cells of waxy maize ear leaves under HS and BR. Ch: chloroplast, GL: granal lamellae, CM: chloroplast membrane, CW: cell wall, P: plastoglobules, To: tonoplast. CK: control, HS: heat stress, BR: 24-epibrassinolide.

Exogenous BR effectively mitigated the heat-induced damage to chloroplast ultrastructure. In SYN5, BR increased the number of chloroplasts per mesophyll cell and lamellae per grana by 12.5% and 73.3%, respectively, relative to HS treatment, along with a increase of 42.6% in grana per unit chloroplast area. YN7 showed a more modest recovery, with increases of 6.3% in chloroplasts per cell and 16.8% in lamellae per grana, resulting in a marginal 2.7% decrease in grana per unit chloroplast area (Table 3, Figure 3). BR also improved membrane integrity, reduced lamellar solubilization, and promoted tighter stacking of grana with clearer outlines. Overall, BR application mitigated the negative impact of HS on chloroplast ultrastructure and enhanced the organizational state of the internal membrane system in waxy maize leaves.

3.6. Photosynthetic Pigment

HS significantly reduced the Chl-a, Chl-b, Chl-a+b, and Car content in ear leaves of two waxy maize hybrids. Exogenous BR significantly attenuated these HS-induced declines (Figure 4; Table S1). The restorative effect of BR on Chl-a under HS was observed in SYN5 at all measured timepoints except 5 DAP in 2024, while in YN7, it was significant only at 5 DAP in 2023 and 15 DAP in 2024 (Figure 4A). A similar pattern was found for Chl-b, which was significantly elevated by BR in SYN5 at 5 and 15 DAP in 2023, and in YN7 at all timepoints except 5 DAP in 2023 (Figure 4B). The reduction in Chl-a+b content was more pronounced in SYN5 than in YN7 under HS (Figure 4C). Mean values across two years revealed declines of 18.0% at 5 DAP and 22.3% at 15 DAP in SYN5 compared to CK versus reductions of 10.1% and 16.8% in YN7, respectively. Notably, BR application under HS significantly restored the Chl-a+b content in both hybrids at 5 and 15 DAP in 2023 and at 15 DAP in 2024 (Figure 4C). Car content dynamics under HS mirrored those of Chl-a (Figure 4D). Critically, SYN5 demonstrated greater HS sensitivity in photosynthetic pigment degradation than YN7, while BR exhibited stronger efficacy in mitigating the pigment loss in SYN5.

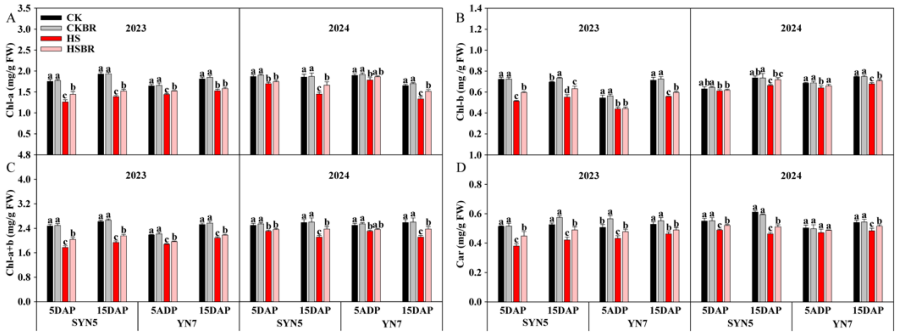

Figure 4. Effects of HS and BR on the pigment content of waxy maize ear leaves. (**A**) Chl-a: chlorophyll a, (**B**) Chl-b: chlorophyll b, (**C**) Chl-a+b: chlorophyll a+b, (**D**) Car: carotenoid. DAP: days after pollination, CK: control, HS: heat stress, BR: 24-epibrassinolide. Different letters indicate significant differences ($p < 0.05$). Error line represents the standard deviation of the mean (n = 3).

3.7. Photosynthetic Key Enzyme Activity

HS significantly inhibited PEPCase and Rubisco activities in ear leaves of both hybrids, while exogenous BR application significantly alleviated these effects (Figure 5; Table S1). Under HS, the PEPCase activity decreased significantly in both hybrids except for SYN5 at 5 DAP in 2024, whereas the Rubisco activity declined significantly except for YN7 at 15 DAP in 2023 and 5 DAP in 2024 (Figure 5). Compared to HS, HSBR significantly increased the PEPCase activity in both hybrids except for SYN5 at 5 DAP in 2024, and it enhanced Rubisco activity except for YN7 at 5 DAP in 2024 (Figure 5). Notably, under CK conditions, exogenous BR induced significant increases in Rubisco activity for SYN5 at 5 DAP in 2023 and PEPCase activity for YN7 at 5 DAP in 2023 along with elevated PEPCase activity for SYN5 at 15 DAP in 2024. Collectively, HS exerted stronger inhibitory effects on both Rubisco and PEPCase activities in SYN5 compared with YN7, while exogenous BR application induced more pronounced promotional effects (Figure 5).

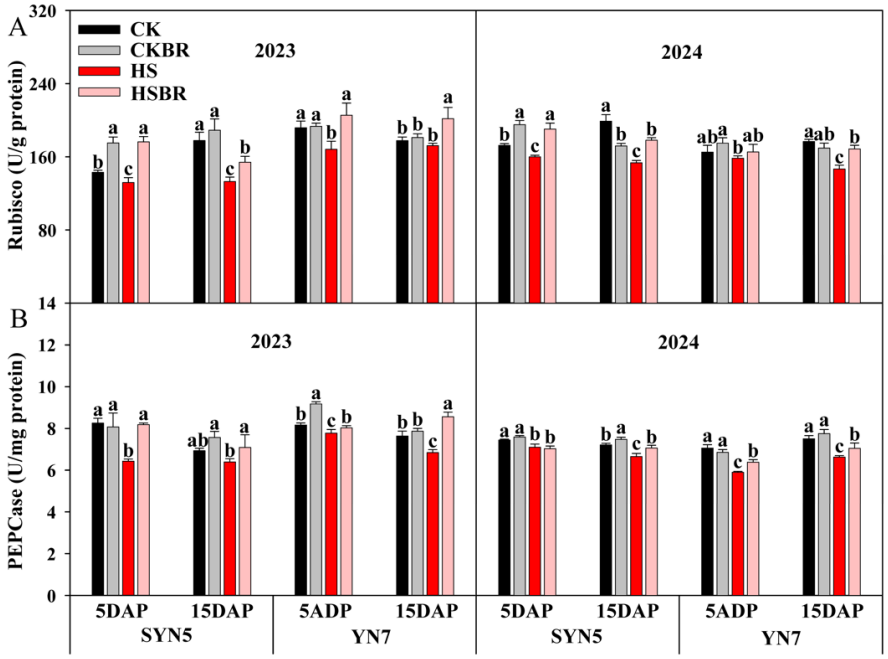

Figure 5. Effects of HS and BR on the photosynthetic related-enzymes activities of waxy maize ear leaves. (**A**) Rubisco: ribulose-1,5-bisphosphate carboxylase/oxygenase, (**B**) PEPCase: phosphoenolpyruvate carboxylase. DAP, days after pollination, CK, control, HS, heat stress, BR: 24-epibrassinolide. Different letters indicate significant differences ($p < 0.05$). Error line represents the standard deviation of the mean (n = 3).

3.8. Antioxidant System

HS significantly inhibited the activities of key antioxidant enzymes (APX, CAT, POD, SOD) in ear leaves of both hybrids, while it significantly increased ROS and H_2O_2 accumulation. Exogenous BR significantly attenuated these HS-induced declines (Figure 6; Table S1). Under HS, APX activity was significantly reduced in both hybrids across most timepoints except for YN7 at 5 DAP in 2023 and SYN5 at 5 DAP in 2024 (Figure 6A). CAT activity responded differently between years: it increased at 5 DAP but decreased at 15 DAP in 2023 while showing significant declines at both timepoints in 2024 (Figure 6B). The POD activity exhibited analogous patterns to APX (Figure 6C). The SOD activity was also considerably diminished by HS, particularly in SYN5 at 15 DAP in 2023 and at both timepoints in 2024, and in YN7 at 5 DAP in 2023 and 15 DAP in 2024 (Figure 6D). Exogenous BR significantly enhanced the activities of all four enzymes under HS.

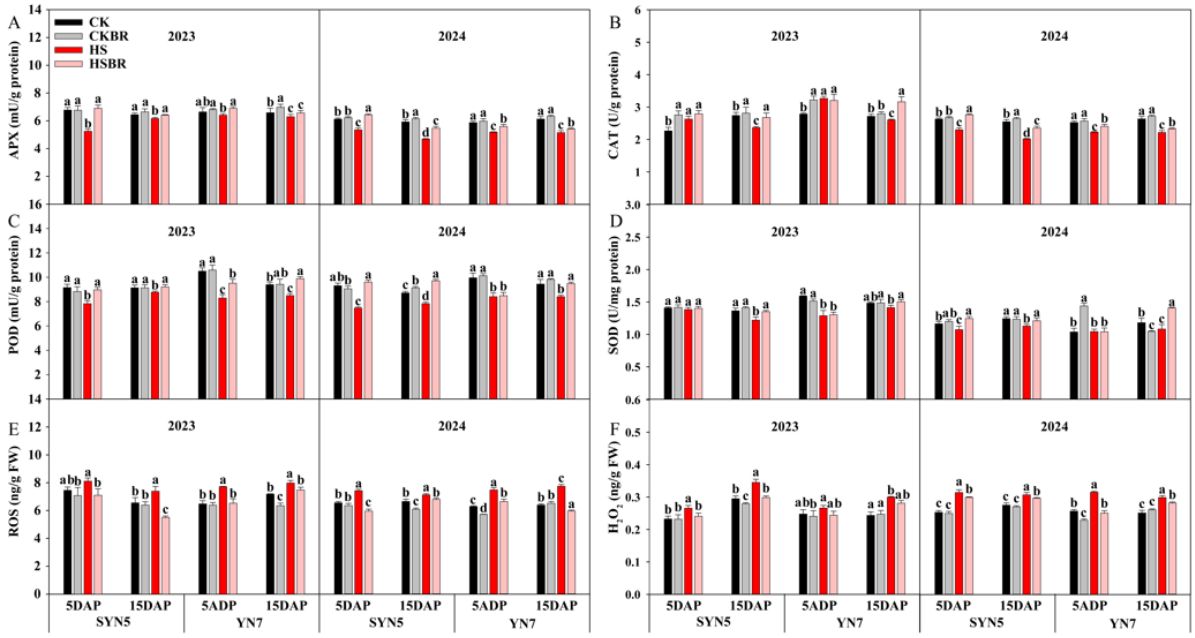

Figure 6. Effects of HS and BR on the antioxidant system of waxy maize ear leaves. (**A**) APX: ascorbate peroxidase, (**B**) CAT: catalase, (**C**) POD: peroxidase, (**D**) SOD: superoxide dismutase, (**E**) ROS: reactive oxygen species, (**F**) H_2O_2: hydrogen peroxide. DAP: days after pollination, CK: control, HS: heat stress, BR: 24-epibrassinolide. Different letters indicate significant differences ($p < 0.05$). Error line represents the standard deviation of the mean (n = 3).

Relative to CK, the ROS content in YN7 under HS increased by 19.0% at 5 DAP and 14.2% at 15 DAP, exceeding the increases observed in SYN5 (11.0% and 9.9%, respectively) (Figure 6E). Likewise, the H_2O_2 content in SYN5 under HS increased by 19.2% at 5 DAP and 14.2% at 15 DAP, respectively, but decreased by 7.1% and 8.5% with exogenous BR application (Figure 6F). The HSBR treatment effectively reversed this accumulation, reducing ROS and H_2O_2 levels in both hybrids. Notably, the BR-mediated mitigation of this oxidative damage was generally more effective in SYN5 than in YN7.

3.9. Endogenous Hormone Content

HS significantly increased the ABA content but decreased the IAA content in the ear leaves of both hybrids. Exogenous BR significantly mitigated the effects of HS (Figure 7A, Table S1). Under HS, the mean annual ABA content in SYN5 increased by 12.0% at 5 DAP and 9.2% at 15 DAP compared to CK, while the ABA content in YN7 increased by 15.2% at 5 DAP and 13.7% at 15 DAP, respectively (Figure 7A). Concurrently, the IAA content in

SYN5 decreased by 7.7% at 5 DAP and 14.4% at 15 DAP under HS (Figure 7B). The IAA content in YN7 decreased by 10.8% at 5 DAP and 15.4% at 15 DAP, respectively (Figure 7B). Compared to HS, HSBR significantly reduced the ABA content in both hybrids except in YN7 at 5 DAP (Figure 7A). Additionally, HSBR significantly increased the IAA content in SYN5 (except at 15 DAP in 2024) and in YN7 (except at 5 DAP in 2024) (Figure 7B). Notably, YN7 exhibited greater hormonal fluctuations under HS, while BR demonstrated a stronger regulatory effect in this hybrid.

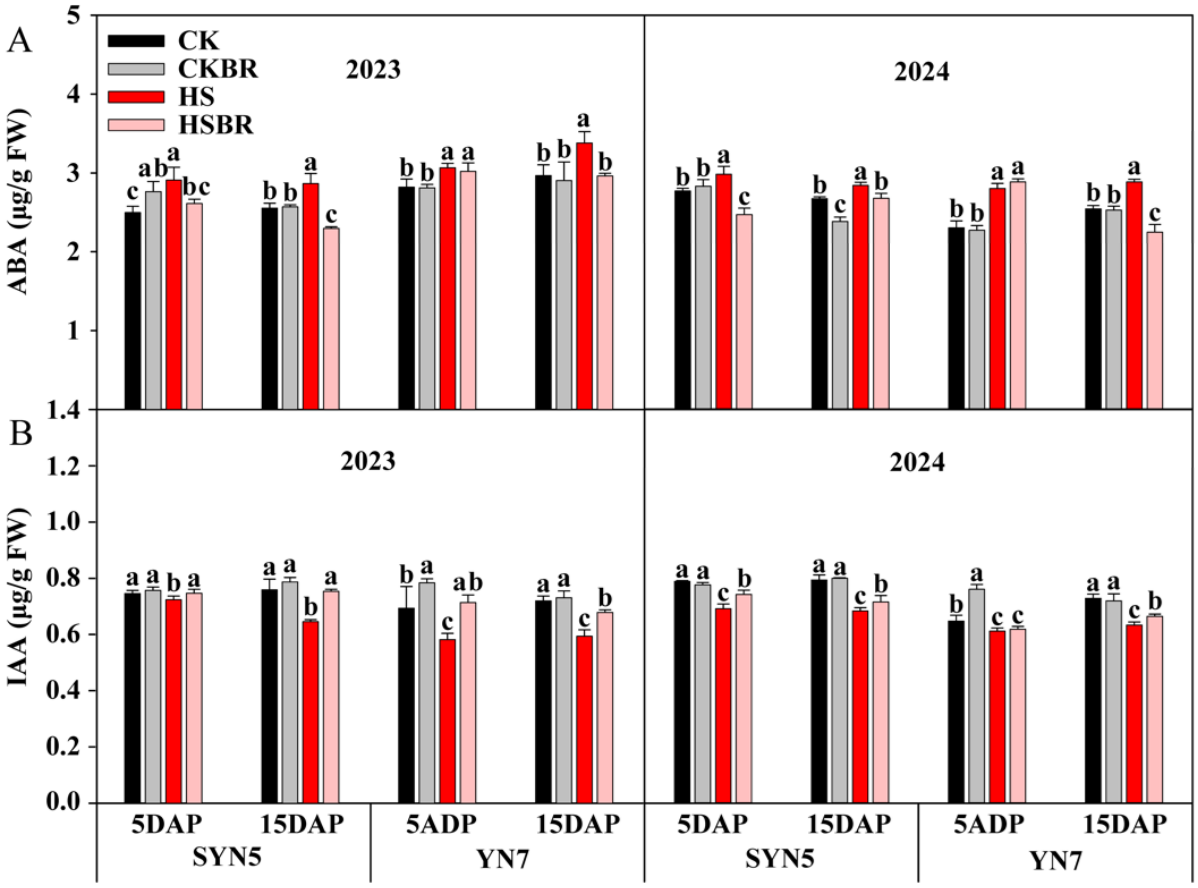

Figure 7. Effects of HS and BR on the antioxidant system of waxy maize ear leaves. (**A**) ABA: abscisic acid content, (**B**) IAA: indole-3-acetic acid. DAP: days after pollination, CK: control, HS: heat stress, BR: 24-epibrassinolide. Different letters indicate significant differences ($p < 0.05$). Error line represents the standard deviation of the mean (n = 3).

3.10. Soluble Protein and Sugar Content

HS induced a significant depletion of soluble protein and sugar in ear leaves, which was effectively counteracted by BR (Figure 8, Table S1). Under HS, the soluble protein content declined by 17.2% at 5 DAP and 8.3% at 15 DAP in SYN5 compared to CK, while YN7 showed a 7.2% reduction at 15 DAP (Figure 8A). Exogenous BR under HS significantly promoted soluble protein content by 12.3% at 5 DAP and 11.6% at 15 DAP in SYN5 and by 8.7% and 7.1% in YN7 (Figure 8A). Similarly, HS decreased soluble sugar content by 10.4% at 5 DAP and 9.3% at 15 DAP in SYN5 and by 14.1% at 5 DAP and 13.7% at 15 DAP in YN7. HSBR restored soluble sugar accumulation, increasing content by 4.3% at 5 DAP and 5.4% at 15 DAP in SYN5, and by 7.4% and 4.8% in YN7 compared to HS (Figure 8B). Notably, YN7 showed greater HS-induced declines in both soluble protein and sugar than SYN5 with BR eliciting stronger compensatory increases in this hybrid.

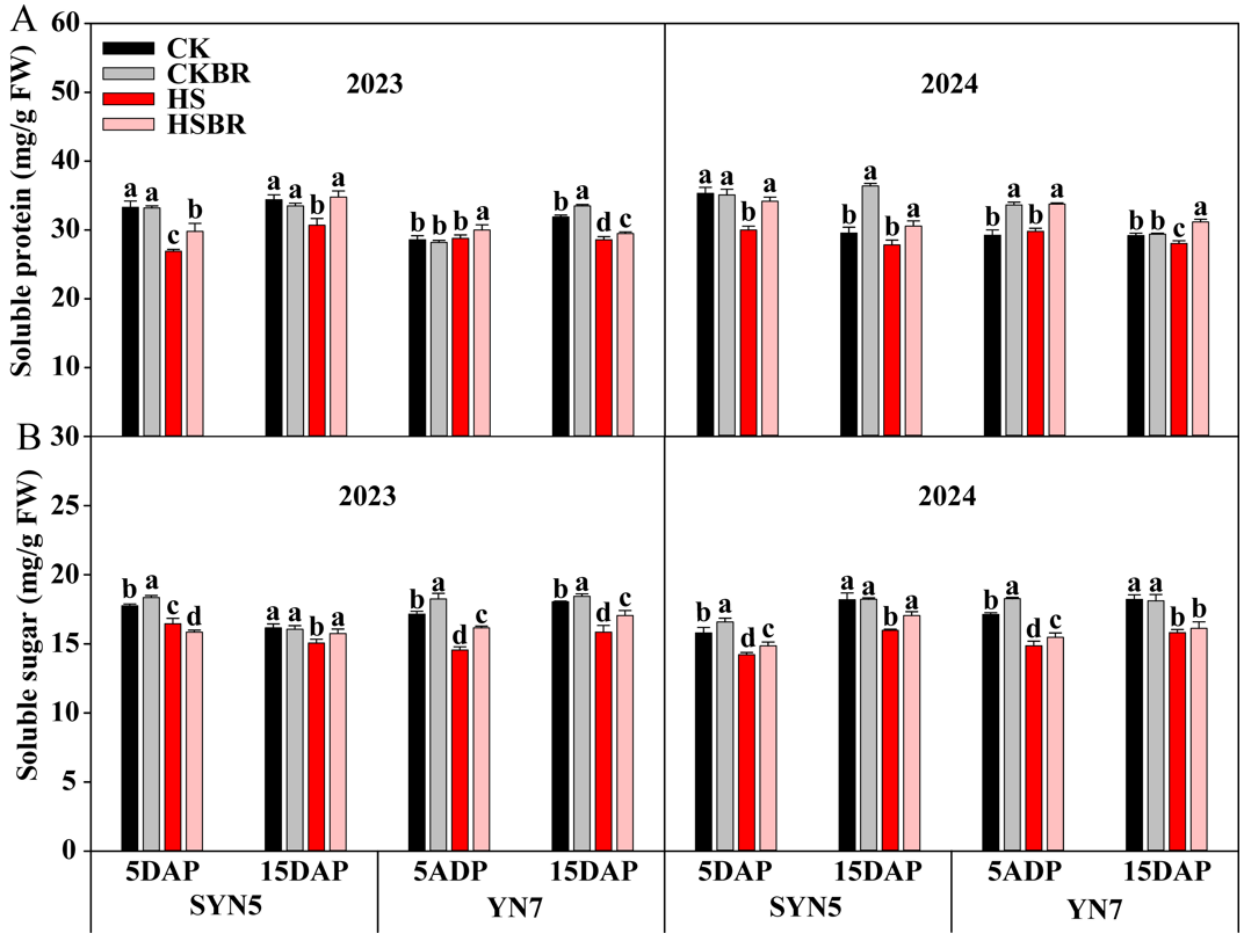

Figure 8. Effects of HS and BR on the antioxidant system of waxy maize ear leaves. (**A**) Soluble protein content, (**B**) soluble sugar content. DAP: days after pollination, CK: control, HS: heat stress, BR: 24-epibrassinolide. Different letters indicate significant differences ($p < 0.05$). Error line represents the standard deviation of the mean (n = 3).

4. Discussion

4.1. Effects of Exogenous BR on the Yield, Dry Matter Accumulation and Translocation of Waxy Maize Under HS

Dry matter accumulation, translocation, and partitioning critically determine the yield formation of crops [41,42]. This study confirms a highly significant positive correlation between DMA and yield ($p < 0.01$, Figure 9). Crop productivity is co-determined by pre-anthesis assimilate remobilization and post-anthesis photosynthetic gain [43,44] with stress resilience heavily reliant on efficient reserve mobilization to developing grains [45]. HS impairs yield via dual mechanisms: (1) reducing post-anthesis biomass accumulation [46] and (2) suppressing assimilate translocation through shortened grain-filling duration [47] and diminished non-structural carbohydrate (NSC) remobilization efficiency [48,49], resulting in consequent photosynthate retention in vegetative organs [50,51] and collectively suppressing sink-directed nutrient flux during grain filling. In this study, SYN5 exhibited more pronounced reductions in TAA, CRA, and DMA than YN7 (Table 1 and Table S1). Although SYN5 showed greater increases in TAP, TRP, and CRP, these enhancements failed to compensate for the direct reduction in post-anthesis assimilates. Consequently, SYN5 (−42.8%) incurred significantly larger HS-induced yield losses relative to YN7 (−39.0%) (Figure 1, Table S1).

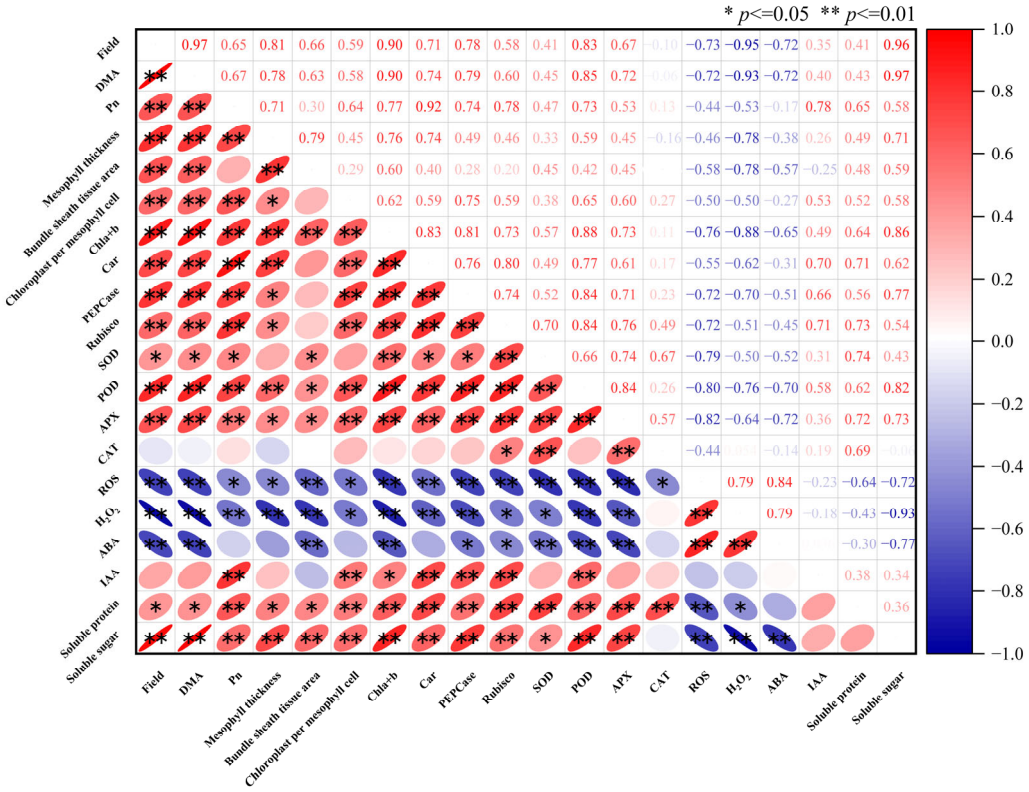

Figure 9. Correlation analysis between field, DMA, and physiological indices in two waxy maize hybrids under HS and BR (Person). DMA: dry matter accumulation after pollination, Pn: net photosynthetic rate, Chl: chlorophyll, Car: carotenoid, PEPCase, phosphoenolpyruvate carboxylase, Rubisco: ribulose-1,5-bisphosphate.

Exogenous BR enhance grain filling by promoting NSC remobilization from stems to kernels, as documented in cereals [52,53]. In HS-tolerant rice, BR elevate both yield components and DMA [54]. Our study demonstrates that BR application under HS reversed DM partitioning alterations: reducing pre-anthesis assimilate translocation while significantly enhancing post-anthesis accumulation and partitioning, ultimately improving grain yield (Figure 1). Importantly, BR efficacy exhibited clear context-dependent and genotype-specific patterns: while effects under CK were minimal; the HS-sensitive hybrid SYN5 showed a markedly stronger response with a 68.5% increase in DMA under HSBR compared to a 38.4% increase in the HS-tolerant hybrid YN7.

4.2. Effects of Exogenous BR on Photosynthetic Performance of Waxy Maize Leaves Under HS

Photosynthesis serves as the foundation of energy metabolism and directly determines crop biomass accumulation [16]. Consistent evidence from summer maize [22], wheat [55] and rice [56] demonstrate that HS suppresses photosynthetic capacity and imposes yield penalties. Our correlation analysis revealed significant positive relationships between Pn and both DMA and yield ($p < 0.01$, Figure 9). HS significantly reduced Pn and Gs while increasing Ci (Figure 2A–C), indicating a non-stomatal limitation of photosynthesis. Critically, diminished Gs restricts evaporative cooling [57], exacerbating thermal damage. As ABA promotes stomatal closure [58,59], CO_2 deprivation enhances photorespiration—diverting metabolic flux toward energy-consuming processes [60,61]. In the present study, BR application counteracted this cascade by suppressing ABA biosynthesis while accelerating its catabolism [62], thereby maintaining stomatal aperture under stress conditions [63] and reducing photorespiratory losses [64].

Photosynthetic pigments are indispensable components of photosynthesis, providing the fundamental basis for light-driven energy conversion [65]. Photosynthetic pigments maintain a balance between synthesis and degradation under optimal conditions [66]. HS disrupts this balance by increasing the number of photosynthetic pigment catabolic enzymes, leading to significant photosynthetic pigment depletion [67]. HS also promotes ABA accumulation, which accelerates Chl degradation and senescence [68,69]. Exogenous BR mitigates ABA accumulation and enhances IAA biosynthesis (Figure 7, Table S1), upregulating key Chl biosynthetic enzymes [70] and promoting photosynthetic pigment accumulation (Figure 4A–C). In C4 maize, photosynthetic carbon fixation relies on the coordinated activities of PEPCase, which catalyzes the initial CO_2 fixation, and Rubisco, which subsequently drives carboxylation in the Calvin cycle [71,72]. HS severely suppressed both enzymes (Figure 5), which is consistent with prior reports [73,74]. Positive correlations existed between Pn and both PEPCase and Rubisco activities ($p < 0.01$; Figure 9). Notably, BR uniquely upregulated PEPCase activity under HS (Figure 5B), mitigating carbon fixation constraints.

4.3. Effects of Exogenous BR on Anatomical Microstructure and Mesophyll Cell Ultrastructure of Waxy Maize Leaves Under HS

Leaf anatomy critically determines photosynthetic performance and exhibits HS sensitivity [75]. Correlation analysis revealed significant positive relationships between Pn and mesophyll thickness ($p < 0.01$, Figure 9). In this study, HS significantly reduced the leaf thickness and vascular bundle tissue area, particularly in SYN5 (Table 2). While thicker leaves enhance light harvesting [76], reduced thickness facilitates convective cooling, representing a trade-off between carbon gain and thermal regulation [77]. Vascular bundles critically determine hydraulic efficiency with larger cross-sectional areas of veins and vascular tissues enhancing the conductance of water and mineral nutrients [78]. However, HS decreased IAA levels in waxy maize ear leaves (Figure 7B, Table S1), disrupting polar auxin transport via the xylem [79]. Conversely, BR application restored IAA accumulation under HS (Figure 7B), which rebalanced hormones and stimulated cell division and expansion, ultimately enhancing leaf anatomical adaptation by increasing leaf thickness and expanding both the bundle sheath area and bundle sheath tissue area (Figure S2, Table 2).

Chloroplasts, essential for photosynthesis, require an intact ultrastructure for optimal function [80]. Chloroplast volume changes, driven by ion flux alterations, can disrupt the cytoplasmic ionic environment and impair the function of neighboring organelles [81]. HS disrupts the stability of protein supercomplexes within thylakoid membranes and increases membrane permeability, thereby perturbing ion homeostasis. To restore osmotic balance, water influx into the thylakoid lumen and chloroplast stroma may occur, ultimately inducing structural swelling [82]. It has been established that chloroplast swelling markedly alters the apparent absorption of green light by altering its optical properties [83]. In addition, heat stress induces the disassembly of thylakoid membranes by impairing their structural integrity, thereby reducing the number of grana and lamellae [84]. These changes, particularly in the SYN5 (Figure 3, Table 3), impair photosynthetic efficiency, since HS disrupts photochemical reactions in thylakoid lamellae and carbon metabolism in the stroma [69]. Notably, the observed changes in the size and abundance of plastoglobules reveal their pivotal role in lipid metabolism and in maintaining chloroplast function under stress conditions [85,86]. Our results showed that BR preserves thylakoid architecture under HS (Figure 3), restoring grana stacking density and membrane continuity (Table 3). BR conferred protection through a dual mechanism: it enhanced H_2O_2 scavenging to prevent oxidative damage to chloroplast membranes [87,88] while also promoting osmolyte accumulation to alleviate HS-induced chloroplast swelling, thereby preserving photosynthetic function [89].

4.4. Effects of Exogenous BR on Antioxidant System and Osmotic Regulators of Waxy Maize Under HS

The detrimental effects of heat stress on plants arise from a twofold nature: direct thermal damage and the consequent oxidative injury. ROS, such as superoxide and H_2O_2, are cytotoxic by-products of metabolic processes that damage membranes and proteins. Antioxidant enzymes like SOD, POD, CAT, and APX maintain ROS homeostasis, improving stress resilience and delaying senescence [90,91]. Under HS, decreased antioxidant enzyme activity leads to ROS accumulation, oxidative damage, and accelerated senescence [92,93]. The levels of ROS and H_2O_2 were negatively correlated with the activities of antioxidant enzymes ($p < 0.01$, Figure 9). Exogenous BR enhances antioxidant activity, reducing ROS and H_2O_2 accumulation (Figure 6) and slowing senescence [94].

Osmotic regulators, including soluble sugars and proteins, play a vital role in stress adaptation by maintaining osmotic balance, scavenging reactive oxygen species (ROS), and stabilizing membrane structures [95–97]. Soluble sugars provide thermotolerance [98], while soluble proteins are essential for stress resilience [99]. The significant positive correlations between soluble sugars, proteins, and ROS levels ($p < 0.01$, Figure 9) likely reflect their concurrent mobilization under stress. Critically, exogenous BR application effectively restored their accumulation (Figure 8), thereby mitigating osmotic stress and supporting a role for BR in enhancing osmotic adjustment [100,101].

5. Conclusions

Heat stress during grain filling severely disrupted yield formation, photosynthetic performance, and redox homeostasis in waxy maize with the hybrid SYN5 showing higher sensitivity. It significantly reduced maturity yield, suppressed photosynthetic parameters (Pn, Gs), degraded chloroplast ultrastructure, diminished antioxidant enzyme activities (APX, CAT, POD, SOD), and elevated ROS and ABA levels. Crucially, exogenous BR application substantially mitigated these deleterious effects: restoring yield, enhancing photosynthetic pigment content (Chl-a+b, Car), preserving chloroplast membrane integrity, reactivating Rubisco/PEPCase activities, and adjusting photosynthetic parameters. BR also alleviated oxidative stress by boosting antioxidant capacity and rebalancing hormones. The stronger restorative effects observed in SYN5 highlight BR's role in reinforcing thermotolerance, particularly in susceptible genotypes. These findings establish BR as an effective strategy for safeguarding waxy maize productivity under heat stress conditions.

Supplementary Materials: The following supporting information can be downloaded at https://www.mdpi.com/article/10.3390/agriculture15232445/s1, Supplementary Figure S1. Daily ambient temperature and precipitation records before treatments in 2023 and 2024. Supplementary Figure S2. Effects of HS and BR on leaf mesophyll anatomy. Supplementary Table S1. Analysis of variance (ANOVA) of dry matter accumulation and translocation, yield, leaf enzyme activity, and substance content.

Author Contributions: Conceptualization, D.L.; methodology, J.L. (Jiawei Liu) and J.L. (Jing Li); software, J.L. (Jiawei Liu); validation, J.G., D.L. and J.L. (Jing Li); formal analysis, J.L. (Jiawei Liu); investigation, G.L. and H.Y.; resources, D.L.; data curation, J.L. (Jiawei Liu); writing—original draft preparation, J.L. (Jiawei Liu); writing—review and editing, J.G.; visualization, J.L. (Jiawei Liu); supervision, J.G.; project administration, D.L.; funding acquisition, D.L. All authors have read and agreed to the published version of the manuscript.

Funding: This work was supported by grants from the National Natural Science Foundation of China (32071958, 32372222), and Priority Academic Program Development of Jiangsu Higher Education Institutions.

Data Availability Statement: Dataset available on request from the authors. The raw data supporting the conclusions of this article will be made available by the authors on request.

Conflicts of Interest: The authors declare no conflicts of interest.

References

1. Bongaarts, J. IPCC, 2023: Climate Change 2023: Synthesis Report. *Popul. Dev. Rev.* **2024**, *50*, 577–580. [CrossRef]
2. Sallam, A.; Amro, A.; El-Akhdar, A.; Dawood, M.F.A.; Kumamaru, T.; Stephen Baenziger, P. Genetic diversity and genetic variation in morpho-physiological traits to improve heat tolerance in Spring barley. *Mol. Biol. Rep.* **2018**, *45*, 2441–2453. [CrossRef]
3. Magana Ugarte, R.; Escudero, A.; Gavilan, R.G. Metabolic and physiological responses of Mediterranean high-mountain and alpine plants to combined abiotic stresses. *Physiol. Plant* **2019**, *165*, 403–412. [CrossRef]
4. Hao, Z.C.; AghaKouchak, A.; Phillips, T.J. Changes in concurrent monthly precipitation and temperature extremes. *Environ. Res. Lett.* **2013**, *8*, 034014. [CrossRef]
5. Liu, B.; Martre, P.; Ewert, F.; Porter, J.R.; Challinor, A.J.; Muller, C.; Ruane, A.C.; Waha, K.; Thorburn, P.J.; Aggarwal, P.K.; et al. Global wheat production with 1.5 and 2.0 °C above pre-industrial warming. *Glob. Change Biol.* **2019**, *25*, 1428–1444. [CrossRef] [PubMed]
6. Khan, A.; Ahmad, M.; Ahmed, M.; Gill, K.S.; Akram, Z. Association analysis for agronomic traits in wheat under terminal heat stress. *Saudi J. Biol. Sci.* **2021**, *28*, 7404–7415. [CrossRef] [PubMed]
7. Tigchelaar, M.; Battisti, D.S.; Naylor, R.L.; Ray, D.K. Future warming increases probability of globally synchronized maize production shocks. *Proc. Natl. Acad. Sci. USA* **2018**, *115*, 6644–6649. [CrossRef]
8. Hou, P.; Liu, Y.E.; Liu, W.M.; Yang, H.S.; Xie, R.Z.; Wang, K.R.; Ming, B.; Liu, G.Z.; Xue, J.; Wang, Y.H.; et al. Quantifying maize grain yield losses caused by climate change based on extensive field data across China. *Resour. Conserv. Recycl.* **2021**, *174*, 105811. [CrossRef]
9. Li, Q.; Wang, P.J.; Li, Y.; Tang, J.X.; Li, X.; Zhang, Y.D.; Han, D.C.; Zhao, Y.C.; Wang, Q.; Yang, Z.Q. Identifying trigger thresholds for heat damage at different growth stages of summer maize: A case study of the Huang-Huai-Hai Plain, China. *Eur. J. Agron.* **2025**, *170*, 127729. [CrossRef]
10. Nelson, O.; Pan, D. Starch synthesis in maize endosperms. In *Annual Review of Plant Biology*; Jones, R.L., Ed.; Annual Review of Plant Physiology and Plant Molecular Biology; Annual Reviews: Palo Alto, CA, USA, 1995; Volume 46, pp. 475–496.
11. Guo, Y.Q.; Sun, L.L.; Chen, L.R.; Wang, X.Y.; Wang, C.G.; Gong, K.J. Applications of waxy corn flour based on physicochemical and processing properties: Comparison with waxy rice flour and waxy corn starch. *Int. J. Food Eng.* **2021**, *17*, 355–363. [CrossRef]
12. Luo, Y.; Han, X.; Shen, M.; Yang, J.; Ren, Y.; Xie, J. *Mesona chinensis* polysaccharide on the thermal, structural and digestibility properties of waxy and normal maize starches. *Food Hydrocoll.* **2021**, *112*, 106317. [CrossRef]
13. Lobell, D.B.; Schlenker, W.; Costa-Roberts, J. Climate trends and global crop production since 1980. *Science* **2011**, *333*, 616–620. [CrossRef]
14. Edreira, J.I.R.; Otegui, M.E. Heat stress in temperate and tropical maize hybrids: Differences in crop growth, biomass partitioning and reserves use. *Field Crops Res.* **2012**, *130*, 87–98. [CrossRef]
15. Chen, L.Q.; Qu, X.Q.; Hou, B.H.; Sosso, D.; Osorio, S.; Fernie, A.R.; Frommer, W.B. Sucrose efflux mediated by SWEET proteins as a key step for phloem transport. *Science* **2012**, *335*, 207–211. [CrossRef] [PubMed]
16. Bommert, P.; Whipple, C. Grass inflorescence architecture and meristem determinacy. *Semin. Cell. Dev. Biol.* **2018**, *79*, 37–47. [CrossRef] [PubMed]
17. Mathur, S.; Allakhverdiev, S.I.; Jajoo, A. Analysis of high temperature stress on the dynamics of antenna size and reducing side heterogeneity of Photosystem II in wheat leaves (*Triticum aestivum*). *BBA-Bioenergetics* **2011**, *1807*, 22–29. [CrossRef]
18. Posch, B.C.; Hammer, J.; Atkin, O.K.; Bramley, H.; Ruan, Y.L.; Trethowan, R.; Coast, O. Wheat photosystem II heat tolerance responds dynamically to short- and long-term warming. *J. Exp. Bot.* **2022**, *73*, 3268–3282. [CrossRef]
19. Huang, H.; Ullah, F.; Zhou, D.X.; Yi, M.; Zhao, Y. Mechanisms of ROS regulation of plant development and stress responses. *Front. Plant Sci.* **2019**, *10*, 800. [CrossRef]
20. Suzuki, N.; Katano, K. Coordination between ROS regulatory systems and other pathways under heat stress and pathogen attack. *Front. Plant Sci.* **2018**, *9*, 490. [CrossRef]
21. Hasanuzzaman, M.; Nahar, K.; Fujita, M. Extreme temperature responses, oxidative stress and antioxidant defense in plants. In *Abiotic Stress—Plant Responses and Applications in Agriculture*; IntechOpen: London, UK, 2013; pp. 169–205.
22. Shao, J.Y.; Wang, Q.H.; Liu, P.; Zhao, B.; Han, W.; Zhang, J.W.; Ren, B.Z. The complex stress of waterlogging and high temperature accelerated maize leaf senescence and decreased photosynthetic performance at different growth stages. *J. Agron. Crop Sci.* **2024**, *210*, e12689. [CrossRef]
23. Lisong, C.; Xinghui, L. Effect of high temperature stress on cell membrane permeability and photosynthetic pigment in leaves of peach and pomelo. *Plant Sci. J.* **1997**, *15*, 233–237.

24. Zhang, P.; Sharwood, R.E.; Carroll, A.; Estavillo, G.M.; von Caemmerer, S.; Furbank, R.T. Systems analysis of long-term heat stress responses in the C_4 grass Setaria viridis. *Plant Cell* **2025**, *37*, 4. [CrossRef] [PubMed]
25. Kan, Y.; Mu, X.R.; Gao, J.; Lin, H.X.; Lin, Y. The molecular basis of heat stress responses in plants. *Mol. Plant* **2023**, *16*, 1612–1634. [CrossRef] [PubMed]
26. Saini, S.; Sharma, I.; Pati, P.K. Versatile roles of brassinosteroid in plants in the context of its homoeostasis, signaling and crosstalks. *Front. Plant Sci.* **2015**, *6*, 950. [CrossRef]
27. Tanveer, M.; Shahzad, B.; Sharma, A.; Khan, E.A. 24-Epibrassinolide application in plants: An implication for improving drought stress tolerance in plants. *Plant Physiol. Biochem.* **2019**, *135*, 295–303. [CrossRef]
28. Hussain, M.A.; Fahad, S.; Sharif, R.; Jan, M.F.; Mujtaba, M.; Ali, Q.; Ahmad, A.; Ahmad, H.; Amin, N.; Ajayo, B.S.; et al. Multifunctional role of brassinosteroid and its analogues in plants. *Plant Growth Regul.* **2020**, *92*, 141–156. [CrossRef]
29. Sadura, I.; Janeczko, A. Brassinosteroids and the tolerance of cereals to low and high temperature stress: Photosynthesis and the physicochemical properties of cell membranes. *Int. J. Mol. Sci.* **2022**, *23*, 342. [CrossRef]
30. Zhang, J.; Zhang, Y.; Khan, R.; Wu, X.Y.; Zhou, L.; Xu, N.; Du, S.S.; Ma, X.H. Exogenous application of brassinosteroids regulates tobacco leaf size and expansion via modulation of endogenous hormones content and gene expression. *Physiol. Mol. Biol. Plants* **2021**, *27*, 847–860. [CrossRef]
31. Rattan, A.; Kapoor, D.; Kapoor, N.; Bhardwaj, R.; Sharma, A. Brassinosteroids regulate functional components of antioxidative defense system in salt stressed maize seedlings. *J. Plant Growth Regul.* **2020**, *39*, 1465–1475. [CrossRef]
32. Ahammed, G.J.; Li, X.; Liu, A.R.; Chen, S.C. Brassinosteroids in plant tolerance to abiotic stress. *J. Plant Growth Regul.* **2020**, *39*, 1451–1464. [CrossRef]
33. Sharma, P.; Kumar, A.; Bhardwaj, R. Plant steroidal hormone epibrassinolide regulate—Heavy metal stress tolerance in *Oryza sativa* L. by modulating antioxidant defense expression. *Environ. Exp. Bot.* **2016**, *122*, 1–9. [CrossRef]
34. Yin, Y.; Qin, K.; Song, X.; Zhang, Q.; Zhou, Y.; Xia, X.; Yu, J. BZR1 transcription factor regulates heat stress tolerance through FERONIA receptor-like kinase-mediated reactive oxygen species signaling in tomato. *Plant Cell Physiol.* **2018**, *59*, 2239–2254. [CrossRef] [PubMed]
35. Dhaubhadel, S.; Browning, K.S.; Gallie, D.R.; Krishna, P. Brassinosteroid functions to protect the translational machinery and heat-shock protein synthesis following thermal stress. *Plant J.* **2002**, *29*, 681–691. [CrossRef] [PubMed]
36. Zhao, G.; Xu, H.; Zhang, P.; Su, X.; Zhao, H. Effects of 2,4-epibrassinolide on photosynthesis and Rubisco activase gene expression in *Triticum aestivum* L. seedlings under a combination of drought and heat stress. *Plant Growth Regul.* **2016**, *81*, 377–384. [CrossRef]
37. Quintero-CalderÓN, E.H.; SÁNchez-Reinoso, A.D.; ChÁVez-Arias, C.C.; Garces-Varon, G.; Restrepo-DÍAz, H. Rice seedlings showed a higher heat tolerance through the foliar application of biostimulants. *Not. Bot. Horti. Agrobot.* **2021**, *49*, 12120. [CrossRef]
38. Gao, Z.; Liang, X.-G.; Zhang, L.; Lin, S.; Zhao, X.; Zhou, L.-L.; Shen, S.; Zhou, S.-L. Spraying exogenous 6-benzyladenine and brassinolide at tasseling increases maize yield by enhancing source and sink capacity. *Field Crops Res.* **2017**, *211*, 1–9. [CrossRef]
39. Wang, X.; Cai, J.; Liu, F.L.; Jin, M.; Yu, H.X.; Jiang, D.; Wollenweber, B.; Dai, T.B.; Cao, W.X. Pre-anthesis high temperature acclimation alleviates the negative effects of post-anthesis heat stress on stem stored carbohydrates remobilization and grain starch accumulation in wheat. *J. Cereal Sci.* **2012**, *55*, 331–336. [CrossRef]
40. Arnon, D.I. Copper enzymes in isolated chloroplasts. polyphenoloxidase in beta vulgaris. *Plant Physiol.* **1949**, *24*, 1–15. [CrossRef]
41. Saıdou, A.; Janssen, B.H.; Temminghoff, E.J.M. Effects of soil properties, mulch and NPK fertilizer on maize yields and nutrient budgets on ferralitic soils in southern Benin. *Agric. Ecosyst. Environ.* **2003**, *100*, 265–273. [CrossRef]
42. Wang, W.; Cai, C.; Lam, S.K.; Liu, G.; Zhu, J. Elevated CO_2 cannot compensate for japonica grain yield losses under increasing air temperature because of the decrease in spikelet density. *Eur. J. Agron.* **2018**, *99*, 21–29. [CrossRef]
43. Yang, J.; Zhang, J. Grain filling of cereals under soil drying. *New Phytol.* **2006**, *169*, 223–236. [CrossRef]
44. McIntyre, C.L.; Seung, D.; Casu, R.E.; Rebetzke, G.J.; Shorter, R.; Xue, G.P. Genotypic variation in the accumulation of water soluble carbohydrates in wheat. *Funct. Plant Biol.* **2012**, *39*, 560–568. [CrossRef] [PubMed]
45. Tatar, Ö.; Brück, H.; Asch, F. Photosynthesis and remobilization of dry matter in wheat as affected by progressive drought stress at stem elongation stage. *J. Agron. Crop Sci.* **2016**, *202*, 292–299. [CrossRef]
46. Qi, Y.; Zhang, Q.; Hu, S.J.; Wang, R.Y.; Wang, H.L.; Zhang, K.; Zhao, H.; Ren, S.X.; Yang, Y.; Zhao, F.N.; et al. Effects of high temperature and drought stresses on growth and yield of summer maize during grain filling in north China. *Agriculture* **2022**, *12*, 1948. [CrossRef]
47. Arshad, M.S.; Farooq, M.; Asch, F.; Krishna, J.S.V.; Prasad, P.V.V.; Siddique, K.H.M. Thermal stress impacts reproductive development and grain yield in rice. *Plant Physiol. Biochem.* **2017**, *115*, 57–72. [CrossRef]
48. Zhen, F.X.; Zhou, J.J.; Mahmood, A.; Wang, W.; Chang, X.N.; Liu, B.; Liu, L.L.; Cao, W.X.; Zhu, Y.; Tang, L. Quantifying the effects of short-term heat stress at booting stage on nonstructural carbohydrates remobilization in rice. *Crop J.* **2020**, *8*, 194–212. [CrossRef]
49. Zamani, M.M.; Nabipour, M.; Meskarbashee, M. Stem water soluble carbohydrate remobilization in wheat under heat stress during the grain filling. *Int. J. Agric. Biol.* **2014**, *16*, 401–405.

50. Farooq, M.; Bramley, H.; Palta, J.A.; Siddique, K.H.M. Heat stress in wheat during reproductive and grain-filling phases. *Crit. Rev. Plant Sci.* **2011**, *30*, 491–507. [CrossRef]
51. De la Haba, P.; De la Mata, L.; Molina, E.; Agüera, E. High temperature promotes early senescence in primary leaves of sunflower (*Helianthus annuus* L.) plants. *Can. J. Plant Sci.* **2014**, *94*, 659–669. [CrossRef]
52. Lv, X.K.; Li, T.; Wen, X.X.; Liao, Y.C.; Liu, Y. Effect of potassium foliage application post-anthesis on grain filling of wheat under drought stress. *Field Crops Res.* **2017**, *206*, 95–105. [CrossRef]
53. Lv, X.K.; Han, J.; Liao, Y.C.; Liu, Y. Effect of phosphorus and potassium foliage application post-anthesis on grain filling and hormonal changes of wheat. *Field Crops Res.* **2017**, *214*, 83–93. [CrossRef]
54. Chen, Y.H.; Chen, H.Z.; Xiang, J.; Zhang, Y.K.; Wang, Z.G.; Zhu, D.F.; Wang, J.K.; Zhang, Y.P.; Wang, Y.L. Rice spikelet formation inhibition caused by decreased sugar utilization under high temperature is associated with brassinolide decomposition. *Environ. Exp. Bot.* **2021**, *190*, 104585. [CrossRef]
55. Li, Q.; Ye, Y.C.; Wang, D.M.; Wang, Y.J.; Zhang, M.; Cai, R.G.; Zhao, G.C.; Yang, Y.S.; Chang, X.H.; Liu, X.W. Temporal dynamics of pre-flowering dry matter remobilization and post-flowering photosynthetic compensation in wheat under combined high temperature and drought stress. *Plant Growth Regul.* **2025**, *105*, 1307–1321. [CrossRef]
56. Ji, D.L.; Xiao, W.H.; Sun, Z.W.; Liu, L.J.; Gu, J.F.; Zhang, H.; Harrison, M.T.; Liu, K.; Wang, Z.Q.; Wang, W.L.; et al. Translocation and distribution of carbon-nitrogen in relation to rice yield and grain quality as affected by high temperature at early panicle initiation stage. *Rice Sci.* **2023**, *30*, 598–612. [CrossRef]
57. Diao, H.; Cernusak, L.A.; Saurer, M.; Gessler, A.; Siegwolf, R.T.W.; Lehmann, M.M. Uncoupling of stomatal conductance and photosynthesis at high temperatures: Mechanistic insights from online stable isotope techniques. *New Phytol.* **2024**, *241*, 2366–2378. [CrossRef]
58. Berens, M.L.; Wolinska, K.W.; Spaepen, S.; Ziegler, J.; Nobori, T.; Nair, A.; Kruler, V.; Winkelmuller, T.M.; Wang, Y.; Mine, A.; et al. Balancing trade-offs between biotic and abiotic stress responses through leaf age-dependent variation in stress hormone cross-talk. *Proc. Natl. Acad. Sci. USA* **2019**, *116*, 2364–2373. [CrossRef]
59. Sierla, M.; Waszczak, C.; Vahisalu, T.; Kangasjarvi, J. Reactive oxygen species in the regulation of stomatal movements. *Plant Physiol.* **2016**, *171*, 1569–1580. [CrossRef]
60. Wang, X.; Cai, X.; Xu, C.; Wang, Q.; Dai, S. Drought-responsive mechanisms in plant leaves revealed by proteomics. *Int. J. Mol. Sci.* **2016**, *17*, 1706. [CrossRef]
61. Walker, B.J.; VanLoocke, A.; Bernacchi, C.J.; Ort, D.R. The costs of photorespiration to food production now and in the future. *Annu. Rev. Plant Biol.* **2016**, *67*, 107–129. [CrossRef]
62. Wang, Q.; Yu, F.; Xie, Q. Balancing growth and adaptation to stress: Crosstalk between brassinosteroid and abscisic acid signaling. *Plant Cell Environ.* **2020**, *43*, 2325–2335. [CrossRef]
63. Wang, Z.; Zheng, P.; Meng, J.; Xi, Z. Effect of exogenous 24-epibrassinolide on chlorophyll fluorescence, leaf surface morphology and cellular ultrastructure of grape seedlings (*Vitis vinifera* L.) under water stress. *Acta Physiol. Plant.* **2014**, *37*, 1729. [CrossRef]
64. da Fonseca, S.S.; da Silva, B.R.S.; Lobato, A.K.d.S. 24-Epibrassinolide positively modulate leaf structures, antioxidant system and photosynthetic machinery in rice under simulated acid rain. *J. Plant Growth Regul.* **2020**, *39*, 1559–1576. [CrossRef]
65. Simkin, A.J.; Kapoor, L.; Doss, C.G.P.; Hofmann, T.A.; Lawson, T.; Ramamoorthy, S. The role of photosynthesis related pigments in light harvesting, photoprotection and enhancement of photosynthetic yield in planta. *Photosynth. Res.* **2022**, *152*, 23–42. [CrossRef] [PubMed]
66. Hortensteiner, S. Stay-green regulates chlorophyll and chlorophyll-binding protein degradation during senescence. *Trends Plant Sci.* **2009**, *14*, 155–162. [CrossRef]
67. Wang, Q.L.; Chen, J.H.; He, N.Y.; Guo, F.Q. Metabolic reprogramming in chloroplasts under heat stress in plants. *Int. J. Mol. Sci.* **2018**, *19*, 849. [CrossRef]
68. Huang, P.; Li, Z.; Guo, H. New advances in the regulation of leaf senescence by classical and peptide hormones. *Front. Plant Sci.* **2022**, *13*, 923136. [CrossRef]
69. Jespersen, D.; Zhang, J.; Huang, B.R. Chlorophyll loss associated with heat-induced senescence in bentgrass. *Plant Sci.* **2016**, *249*, 1–12. [CrossRef]
70. Siddiqui, H.; Hayat, S.; Bajguz, A. Regulation of photosynthesis by brassinosteroids in plants. *Acta Physiol. Plant.* **2018**, *40*, 59. [CrossRef]
71. Dias, M.C.; Brüggemann, W. Differential inhibition of photosynthesis under drought stress in species with different degrees of development of the C_4 syndrome. *Photosynthetica* **2007**, *45*, 75–84. [CrossRef]
72. von Caemmerer, S.; Hendrickson, L.; Quinn, V.; Vella, N.; Millgate, A.G.; Furbank, R.T. Reductions of Rubisco activase by antisense RNA in the C_4 plant *Flaveria bidentis* reduces Rubisco carbamylation and leaf photosynthesis. *Plant Physiol.* **2005**, *137*, 747–755. [CrossRef]
73. Galmes, J.; Aranjuelo, I.; Medrano, H.; Flexas, J. Variation in Rubisco content and activity under variable climatic factors. *Photosynth. Res.* **2013**, *117*, 73–90. [CrossRef] [PubMed]

74. Hu, J.; Zhao, X.Y.; Gu, L.M.; Liu, P.; Zhao, B.; Zhang, J.W.; Ren, B.Z. The effects of high temperature, drought, and their combined stresses on the photosynthesis and senescence of summer maize. *Agric. Water Manag.* **2023**, *289*, 108525. [CrossRef]
75. Fujii, S.; Nishida, K.; Akitsu, T.K.; Kume, A.; Hanba, Y.T. Variation in leaf mesophyll anatomy of fern species imposes significant effects on leaf gas exchange, light capture, and leaf hydraulic conductance. *Photosynthetica* **2023**, *61*, 225–235. [CrossRef] [PubMed]
76. Klich, M.G. Leaf variations in Elaeagnus angustifolia related to environmental heterogeneity. *Environ. Exp. Bot.* **2000**, *44*, 171–183. [CrossRef]
77. Hao, L.; Guo, L.; Li, R.; Cheng, Y.; Huang, L.; Zhou, H.; Xu, M.; Li, F.; Zhang, X.; Zheng, Y. Responses of photosynthesis to high temperature stress associated with changes in leaf structure and biochemistry of blueberry (*Vaccinium corymbosum* L.). *Sci. Hortic.* **2019**, *246*, 251–264. [CrossRef]
78. Aguraijuja, K.; Kloseiko, J.; Ots, K.; Lukjanova, A. Effect of wood ash on leaf and shoot anatomy, photosynthesis and carbohydrate concentrations in birch on a cutaway peatland. *Environ. Monit. Assess.* **2015**, *187*, 444. [CrossRef]
79. Vedenicheva, N.; Futorna, O.; Shcherbatyuk, M.; Kosakivska, I. Effect of seed priming with zeatin on *Secale cereale* L. growth and cytokinins homeostasis under hyperthermia. *J. Crop Improv.* **2021**, *36*, 656–674. [CrossRef]
80. Flori, S.; Jouneau, P.-H.; Bailleul, B.; Gallet, B.; Estrozi, L.F.; Moriscot, C.; Bastien, O.; Eicke, S.; Schober, A.; Bártulos, C.R.; et al. Plastid thylakoid architecture optimizes photosynthesis in diatoms. *Nat. Commun.* **2017**, *8*, 15885. [CrossRef]
81. Packer, L.; Siegenthaler, P.A.; Nobel, P.S. Light-induced volume changes in spinach chloroplasts. *J. Cell Biol.* **1965**, *26*, 593–599. [CrossRef]
82. Gounaris, K.; Brain, A.R.R.; Quinn, P.J.; Williams, W.P. Structural reorganisation of chloroplast thylakoid membranes in response to heat-stress. *BBA–Bioenergetics* **1984**, *766*, 198–208. [CrossRef]
83. Zhang, R.; Wise, R.R.; Struck, K.R.; Sharkey, T.D. Moderate heat stress of Arabidopsis thaliana leaves causes chloroplast swelling and plastoglobule formation. *Photosynth. Res.* **2010**, *105*, 123–134. [CrossRef]
84. Ben Salem-Fnayou, A.; Bouamama, B.; Ghorbel, A.; Mliki, A. Investigations on the leaf anatomy and ultrastructure of grapevine (*vitis vinifera*) under heat stress. *Microsc. Res. Tech.* **2011**, *74*, 756–762. [CrossRef] [PubMed]
85. Devadasu, E.; Susanto, F.A.; Schilmiller, A.L.; Mahey, M.; Johnny, C.; Lundquist, P.K. Dynamic changes to the plastoglobule lipidome and proteome in maize during heat stress and recovery. *J. Exp. Bot.* **2025**, eraf452. [CrossRef] [PubMed]
86. Espinoza-Corral, R.; Schwenkert, S.; Lundquist, P.K. Molecular changes of Arabidopsis thaliana plastoglobules facilitate thylakoid membrane remodeling under high light stress. *Plant J.* **2021**, *106*, 1571–1587. [CrossRef] [PubMed]
87. Gill, M.B.; Cai, K.F.; Zhang, G.P.; Zeng, F.R. Brassinolide alleviates the drought-induced adverse effects in barley by modulation of enzymatic antioxidants and ultrastructure. *Plant Growth Regul.* **2017**, *82*, 447–455. [CrossRef]
88. Lai, H.J.; Li, X.D.; Chen, Y.L.; Liu, Z.X. Mitigating heat-induced yield loss in peanut: Insights into 24-epibrassino-lide-mediated improvement in antioxidant capacity, photosynthesis, and kernel weight. *Field Crops Res.* **2024**, *316*, 109521. [CrossRef]
89. Dobrikova, A.G.; Vladkova, R.S.; Rashkov, G.D.; Todinova, S.J.; Krumova, S.B.; Apostolova, E.L. Effects of exogenous 24-epibrassinolide on the photosynthetic membranes under non-stress conditions. *Plant Physiol. Biochem.* **2014**, *80*, 75–82. [CrossRef]
90. Zhang, J.; Zhang, M.; Tian, S.; Lu, L.; Shohag, M.; Yang, X. Metallothionein 2 (*SaMT2*) from *sedum alfredii* hance confers increased cd tolerance and accumulation in yeast and tobacco. *PLoS ONE* **2014**, *9*, e102750. [CrossRef]
91. Tokarz, P.; Kaarniranta, K.; Blasiak, J. Role of antioxidant enzymes and small molecular weight antioxidants in the pathogenesis of age-related macular degeneration (AMD). *Biogerontology* **2013**, *14*, 461–482. [CrossRef]
92. Mathur, S.; Sharma, M.P.; Jajoo, A. Improved photosynthetic efficacy of maize (*Zea mays*) plants with arbuscular mycorrhizal fungi (AMF) under high temperature stress. *J. Photochem. Photobiol. B* **2018**, *180*, 149–154. [CrossRef]
93. Tiwari, Y.K.; Yadav, S.K. High temperature stress tolerance in maize (*Zea mays* L.): Physiological and molecular mechanisms. *J. Plant Biol.* **2019**, *62*, 93–102. [CrossRef]
94. Ahammed, G.J.; He, B.B.; Qian, X.J.; Zhou, Y.H.; Shi, K.; Zhou, J.; Yu, J.Q.; Xia, X.J. 24-Epibrassinolide alleviates organic pollutants-retarded root elongation by promoting redox homeostasis and secondary metabolism in *Cucumis sativus* L. *Environ. Pollut.* **2017**, *229*, 922–931. [CrossRef] [PubMed]
95. Kohila, S.; Gomathi, R. Adaptive physiological and biochemical response of sugarcane genotypes to high-temperature stress. *Indian J. Plant Physiol.* **2018**, *23*, 245–260. [CrossRef] [PubMed]
96. Zhang, L.; Chang, Q.; Hou, X.; Wang, J.; Chen, S.; Zhang, Q.; Wang, Z.; Yin, Y.; Liu, J. The effect of high-temperature stress on the physiological indexes, chloroplast ultrastructure, and photosystems of two herbaceous peony cultivars. *J. Plant Growth Regul.* **2022**, *42*, 1631–1646. [CrossRef]
97. Luo, J.; Yang, Z.; Zhang, F.; Li, C. Effect of nitrogen application on enhancing high-temperature stress tolerance of tomato plants during the flowering and fruiting stage. *Front. Plant Sci.* **2023**, *14*, 1172078. [CrossRef]
98. Jeandet, P.; Formela-Luboinska, M.; Labudda, M.; Morkunas, I. The role of sugars in plant responses to stress and their regulatory function during development. *Int. J. Mol. Sci.* **2022**, *23*, 5161. [CrossRef]
99. Bao, G.; Tang, W.; He, F.; Chen, W.; Zhu, Y.; Fan, C.; Zhang, M.; Chang, Y.; Sun, J.; Ding, X. Physiological response in the leaf and stolon of white clover under acid precipitation and freeze-thaw stress. *Funct. Plant Biol.* **2019**, *47*, 50–57. [CrossRef]

100. Xu, F.; Xi, Z.M.; Zhang, H.; Zhang, C.J.; Zhang, Z.W. Brassinosteroids are involved in controlling sugar unloading in *Vitis vinifera* 'Cabernet Sauvignon' berries during veraison. *Plant Physiol. Biochem.* **2015**, *94*, 197–208. [CrossRef]
101. Zhang, Z.L.; Ma, X.R.; Tang, D.D.; Chen, Y.D.; Chen, G.; Zou, J.F.; Tan, L.Q.; Tang, Q.; Chen, W. Effects of brassinosteroid on the physiological changes on two varieties of tea plants under salt stress. *Int. J. Mol. Sci.* **2024**, *25*, 13445. [CrossRef]

Disclaimer/Publisher's Note: The statements, opinions and data contained in all publications are solely those of the individual author(s) and contributor(s) and not of MDPI and/or the editor(s). MDPI and/or the editor(s) disclaim responsibility for any injury to people or property resulting from any ideas, methods, instructions or products referred to in the content.